JOURNAL OF PHYSICAL ORGANIC CHEMISTRY
J. Phys. Org. Chem. 2005; **18:** 1032–1041
Published online 13 June 2005 in Wiley InterScience (www.interscience.wiley.com). DOI: 10.1002/poc.966

Supramolecular assemblies of crown-containing 4-styrylpyridine in the presence of metal cations

Y. V. Fedorov,[1]* O. A. Fedorova,[1] E. N. Andryukhina,[1] N. E. Shepel,[1] M. M. Mashura,[1] S. P. Gromov,[1] L. G. Kuzmina,[2] A. V. Churakov,[2] J. A. K. Howard,[3] E. Marmois,[4] J. Oberlé,[4] G. Jonusauskas[4] and M. V. Alfimov[1]

[1]Photochemistry Center of RAS, Novatorov str. 7a, Moscow 119421, Russia
[2]Institute of General and Inorganic Chemistry, RAS, Leninskii pr. 31, Moscow 117907, Russia
[3]Chemistry Department, University of Durham, South Road, Durham DH1 3LE, UK
[4]Centre de Physique Moléculaire Optique et Hertzienne (CPMOH), UMR 5798, Université Bordeaux 1, 351, Cours de la Libération, 33405 Talence, France

Received 20 October 2004; revised 11 March 2005; accepted 29 April 2005

ABSTRACT: Optical and x-ray experiments showed the possibility of studying 4-styrylpyridine with a 15-crown-5 ether fragment to bind metal cations through the participation of two centres: the crown ether moiety and the heterocyclic part. The metal cations studied can be divided into three groups. Alkaline earth metal cations form complexes with the crown ether centre, H^+, Co^{2+} and Cd^{2+} prefer coordination with the N-atom of heterocyclic part and Hg^{2+} cations form complexes through coordination with both binding centres. Copyright © 2005 John Wiley & Sons, Ltd.

KEYWORDS: 4-styrylpyridine; 15-crown-5 ether; ditopic complex formation; alkaline earth metal cations; heavy metal cations; supramolecular assembly; UV–visible spectroscopy; fluorescence; x-ray analysis

INTRODUCTION

Fluorescent molecules linked to the complexing group are very promising systems for ion analysis in industry, biochemistry and environmental monitoring.[1–10] The crown ethers are well-known complexing fragments in fluoroionophores.[11–20] They possess the possibility of structural variety to achieve selectivity and sensitivity in metal ion analysis.

It is known that 4-styrylpyridine can form complexes with salts of Cu^{2+}, Co^{2+}, Cd^{2+} and Zn^{2+} through coordination of the metal cations with the N-atom of the heterocyclic part.[21,22] The composition of the complexes of substituted pyridine depends on the structure of the substituent. Thus, for 4-methylpyridine (MePy) the complex $Co(MePy)_4$ was found[23] and 4-styrylpyridine (StyPy) is able to form the complex $Co(StyPy)_3$.

The combination of 4-styrylpyridine with a crown ether results in the formation of the ditopic receptor **1** (Scheme 1). The 15-crown-5 ether can bind with alkaline earth metal cations, whereas the pyridine part binds transition and heavy metal cations. In this study, the ditopic complex formation of **1** with different types of metal cations (Mg^{2+}, Ba^{2+}, Cd^{2+}, Co^{2+}, Hg^{2+}) and the effect of complex formation on the optical characteristics of molecule were analyzed in details.

**Correspondence to:* Y. V. Fedorov, Photochemistry Center of RAS, Novatorov str. 7a, Moscow 119421, Russia.
E-mail: fedorov@photonics.ru
Contract/grant sponsor: CRDF; *Contract/grant number:* RC2-2344-MO-02.
Contract/grant sponsor: RFBR; *Contract/grant numbers:* 02-03-33058 and 03-03-32849.

RESULTS AND DISCUSSION

UV and NMR spectroscopy studies

It has been found the *E*-isomer of **1** has strong electronic transitions in the near-UV region, as shown in Fig. 1. The addition of alkaline earth metal (Mg, Ba) perchlorates to a solution of **1** in MeCN resulted in hypsochromic shifts of the long-wavelength absorption band and a hypsochromic shift of the fluorescence band, which are evidently due to the formation of complexes of alkaline earth metal cations with crown ether fragment of molecule (Scheme 2, Table 1).

The equilibrium constants for complex formation of **1** with Mg^{2+}, Ba^{2+}, H^+, Cd^{2+} and Hg^{2+} were calculated from the absorption spectra of solutions at constant ligand concentration and varying of metal perchlorate concentrations using the HYPERQUAD program.[24] Four equilibria were taken into account:

$$L + M \overset{K_{11}}{\rightleftharpoons} LM$$

$$2L + M \overset{K_{21}}{\rightleftharpoons} L_2M$$

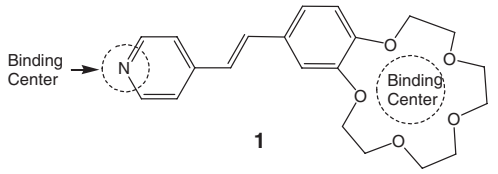

1

Scheme 1

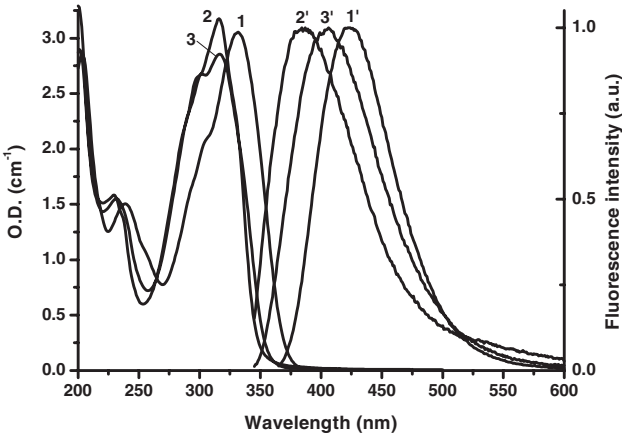

Figure 1. Absorption (1–3) and fluorescence (1′–3′) spectra of dye **1** as free ligand (1, 1′) and as complexes with Mg^{2+} and Ba^{2+}. All spectra were recorded in MeCN at $[\mathbf{1}] = 1.2 \times 10^{-4}$ M, $[Mg^{2+}] = 2.4 \times 10^{-4}$ M (2, 2′), $[Ba^{2+}] = 2.4 \times 10^{-4}$ M (3, 3′); $\lambda_{exc} = 300$ nm

$$2L + 2M \overset{K_{22}}{\rightleftharpoons} L_2M_2$$

$$2L + 3M \overset{K_{23}}{\rightleftharpoons} L_2M_3$$

As one can conclude from the data in Table 1 for **1**, Mg^{2+} cation forms an inclusion complex [**1**·Mg^{2+}] and its stability is usual for this type of crown ether fragment. The addition of Mg^{2+} cations to the dye solution causes a downfield shift of the proton signals in the NMR spectrum of **1** (Table 2). The most pronounced changes were found for the proton signals of the methylene groups of the crown ether fragment.

In the case of Ba^{2+}, the sandwich complex formed possesses high stability. According to the NMR study, the molecules of dye are arranged in a 'head-to-head' stack in the sandwich complex [$\mathbf{1}_2$·Ba^{2+}] (Scheme 2, Table 2). This conclusion was drawn based on upfield shifts of aromatic proton signals in the sandwich complex in comparison with the free ligand (Table 2). The changes in NMR spectra can arise as a result of ring-current effects from the adjacent conjugated molecules.

Table 1. Steady-state absorption data and stability constants for **1** and its complexes with Mg^{2+}, Ba^{2+}, Cd^{2+}, Hg^{2+} and H^+ in MeCN

Compound	λ^{abs} (nm)	$\varepsilon \times 10^{-4}$ ($l\,mol^{-1}\,cm^{-1}$)	Log*K*
1	330	2.53	
1·Mg^{2+}	317	2.60	$\log K_{11} = 5.98 \pm 0.01$
$\mathbf{1}_2$·Ba^{2+}	319	4.66	$\log K_{21} = 10.62 \pm 0.04$
1·Cd^{2+}	355	2.55	$\log K_{11} = 4.21 \pm 0.06$
$\mathbf{1}_2$·Cd^{2+}	355	—	$\log K_{21} = 8.93 \pm 0.14$
$\mathbf{1}_2$·Hg^{2+}	383	5.77	$\log K_{21} = 13.49 \pm 0.28$
$\mathbf{1}_2$·$(Hg^{2+})_2$	370	—	$\log K_{22} = 16.20 \pm 0.33$
$\mathbf{1}_2$·$(Hg^{2+})_3$	376	5.46	$\log K_{23} = 18.19 \pm 0.34$
$(\mathbf{1}_2 \cdot Hg^{2+})_2 \cdot Ba^{2+}$	375	7.61	$\log K_{421} = 37.45 \pm 0.09$
$(\mathbf{1}_2 \cdot Hg^{2+})_2 \cdot (Ba^{2+})_2$	358	9.65	$\log K_{422} = 41.86 \pm 0.09$
1·H^+	400	2.48	$\log K_{11} > 7$

The addition of $HClO_4$ to a solution of **1** in MeCN resulted in the perchlorate salt of **1**, whose long-wavelength absorption band is bathochromically shifted relatively to free ligand **1** (Scheme 3, Figure 2).

The addition of Cd^{2+} or Hg^{2+} perchlorates to the ligand **1** solutions in MeCN leads to changes in UV spectrum similar to those observed in the case of proton addition. Several types of complexes of **1** with Cd^{2+} or Hg^{2+} perchlorates were found. The stability constants of complexes are indicated in Table 1 and the UV and emission spectra are shown in Figs 3 and 4. The formation of complexes [$\mathbf{1}_2$·Cd^{2+}] and [$\mathbf{1}_2$·Hg^{2+}] takes place through the interaction of metal cations with the heterocyclic part of **1**. Additional support for the coordination of metal cations through the heterocyclic part of **1** was found from an NMR study. As one can see from the data in Table 2, the addition of the Cd^{2+} to the **1** solution in CD_3CN causes changes in the position of the proton signals of the aromatic part, whereas the position of the methylene proton signals remains practically unchanged.

At high concentration of Cd^{2+}, the formation of complex [**1**·Cd^{2+}] was observed (Scheme 4). The formation of this complex is accompanied by an additional bathochromic shift of the long-wavelength absorption band. Presumably the interaction of Cd^{2+} with the only pyridine residue results in a more pronounced influence of the cation on the electronic structure of the complex.

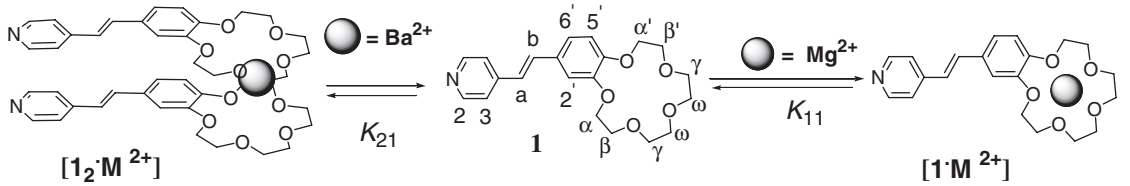

Scheme 2

Table 2. Proton chemical shifts of ligand **1**[a] and its complexes with $Mg(ClO_4)_2$ (25 °C), $Ba(ClO_4)_2$ (60 °C) and $Cd(ClO_4)_2$ (25 °C) in CD_3CN

Compound	**1**:M^{2+} ratio	δ_H (ppm) (aromatic part)						
		H-2,6	H-3,5	H-a	H-b	H-2′	H-5′	H-6′
1		8.50	7.52	7.38	7.05	7.23	6.96	7.15
1·Mg^{2+}	1:2	8.51	7.63	7.51	7.17	7.40	7.22	7.40
$\Delta\delta_{Mg}$[b]		0.01	0.11	0.13	0.12	0.17	0.26	0.25
$\mathbf{1}_2$·Ba^{2+}	2:1	8.39	7.27	7.22	6.92	6.86	6.88	7.19
$\Delta\delta_{Ba}$[b]		−0.11	−0.25	−0.16	−0.13	−0.37	−0.08	0.04
$\mathbf{1}_2$·Cd^{2+}		8.58	7.68	7.48	7.09	7.28	6.99	7.15
$\Delta\delta_{Cd}$[b]		0.08	0.16	0.10	0.04	0.05	0.03	0.00

		δ_H (ppm) (aliphatic part)					
		H-α	H-α'	H-β	H-β'	H-γ,γ'	H-δ,δ'
1		4.11	4.12	3.84	3.84	3.67	3.66
1·Mg^{2+}	1:2	4.18	4.53	4.03	3.97	3.67	3.67
$\Delta\delta_{Mg}$[b]		0.07	0.41	0.19	0.13	0.00	0.01
$\mathbf{1}_2$·Ba^{2+}	2:1	4.29	4.29	4.13	4.13	4.00	3.94
$\Delta\delta_{Ba}$[b]		0.18	0.17	0.29	0.29	0.33	0.28
$\mathbf{1}_2$·Cd^{2+}	2:1	4.10	4.06	3.77	3.77	3.61	3.61
$\Delta\delta_{Cd}$[b]		−0.01	−0.06	−0.07	−0.07	−0.06	−0.05

[a] $C_{\mathbf{1}} = 2 \times 10^{-3}$ M.
[b] $\Delta\delta_M = \delta$(complexed **1**) − δ(free **1**) (ppm).

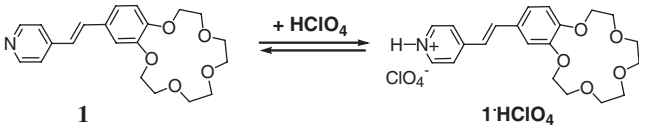

Scheme 3

More complicated complex formation was found for **1** with Hg^{2+} cations. First the complex [$\mathbf{1}_2$·Hg^{2+}] was formed on addition of Hg^{2+} to a solution of **1**. The formation of the complex [$\mathbf{1}_2$·Hg^{2+}] is accompanied by a bathochromic shift of the long-wavelength absorption band in comparison with pure ligand **1**. On increasing the Hg^{2+} concentration, a hypsochromic shift of the long-wavelength absorption band was observed, obviously due to the interaction of Hg^{2+} cations with the crown ether moiety (Fig. 4). The formation of complexes [$\mathbf{1}_2$·Hg_2^{2+}], [$\mathbf{1}_2$·Hg_3^{2+}] and then [**1**·Hg_2^{2+}] could be expected (Scheme 5). It is hardly possible to calculate the values of the stability constants for all these complexes from spectrophotometric titration data. In fact, only the stability constants of complexes [$\mathbf{1}_2$·Hg_2^{2+}] and [$\mathbf{1}_2$·Hg_3^{2+}] were determined with relatively low accuracy (Table 1).

Finally, we prepared mixed complexes when barium perchlorate was added to the solution of complex [$\mathbf{1}_2$·Hg^{2+}]. The long-wavelength absorption band of mixed complexes is shifted to the short-wavelength

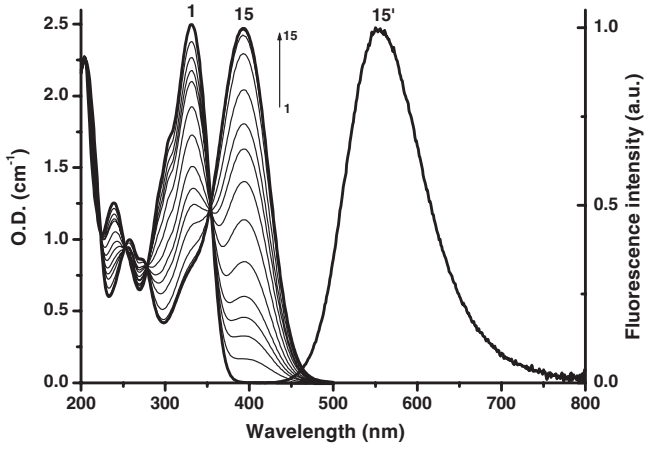

Figure 2. Variation of 1.0×10^{-4} M dye **1** absorption spectra with increasing [$HClO_4$], (1–15)–0–1.4×10^{-4} M, and fluorescence spectra of complex [**1**·$HClO_4$] (15′) in MeCN

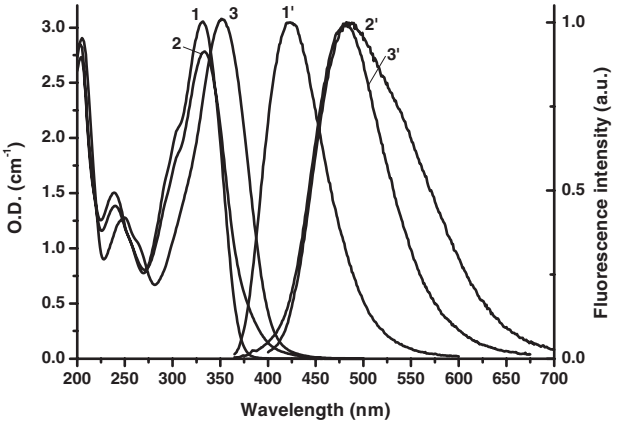

Figure 3. Absorption (1–3) and fluorescence (1′–3′) spectra of dye **1** as free ligand (1, 1′) and as complexes with Cd^{2+}. All spectra were recorded in MeCN at [**1**] = 1.2×10^{-4} M, [Cd^{2+}] = 2.4×10^{-4} M (2, 2′), [Cd^{2+}] = 1.6×10^{-2} M (3, 3′); λ_{exc} = 400 nm

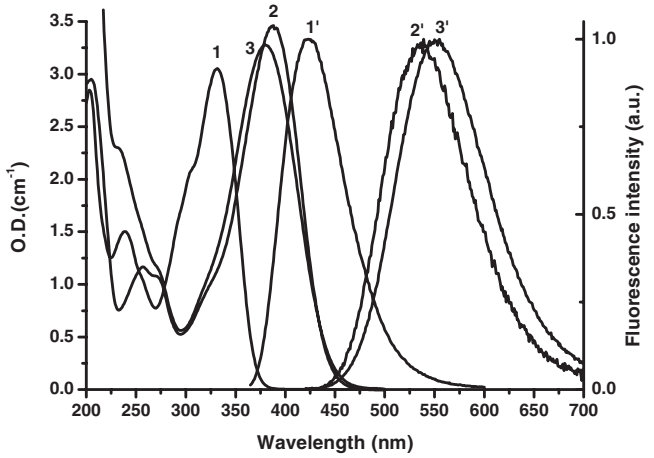

Figure 4. Absorption (1–3) and fluorescence (1′–3′) spectra of dye **1** as free ligand (1, 1′) and as complexes with Hg^{2+}. All spectra were recorded in MeCN at $[\mathbf{1}] = 1.2 \times 10^{-4}$ M, $[Hg^{2+}] = 2.4 \times 10^{-4}$ M (2, 2′), $[Hg^{2+}] = 2.4 \times 10^{-2}$ M (3, 3′)

region relative to that of the $[\mathbf{1}_2 \cdot Hg^{2+}]$ complex and to the long-wavelength region relative to that of the $[\mathbf{1}_2 \cdot Ba^{2+}]$ complex (Table 1). Bearing in mind the strong preference for barium cations to form sandwich complexes with benzo-15-crown-5, the formation of complexes as presented in Scheme 6 could be suggested. The results of the spectrophotometric titration of complex $[\mathbf{1}_2 \cdot Hg^{2+}]$ with barium perchlorate confirm this possibility. The stability constants for complexes $[\mathbf{1}_4 \cdot (Hg^{2+})_2\ Ba^{2+}]$ and $[\mathbf{1}_4 \cdot (Hg^{2+})_2\ (Ba^{2+})_2]$ were calculated at a fixed value of the stability constant for complex $[\mathbf{1}_2 \cdot Hg^{2+}]$ (Table 1).

The explanation for hypso- or bathochromic shifts on complex formation in crown-containing stilbene-like molecules has been presented in detail.[25–27] When a fluorophore contains an electron-donating group conjugated to an electron-withdrawing group, it undergoes intramolecular charge transfer from the donor to acceptor upon excitation by light. It can therefore be anticipated that cations in close interaction with the donor or acceptor moiety will affect the efficiency of intramolecular charge transfer. When a group playing the role of an electron donor interacts with a cation, the latter reduces the electron-donating character of the group, owing to the resulting reduction in conjugation, and a blue shift of the absorption spectrum is expected together with a decrease in extinction coefficient. Conversely, a cation interaction with an acceptor group enhances the electron-withdrawing character of the group and the absorption spectrum is therefore red shifted.

Investigations by fluorescence method

The fluorescence peak wavelengths, quantum yields and lifetimes for **1** alone and **1** complexes with Mg^{2+}, Ba^{2+}, Cd^{2+}, Hg^{2+}, H^+ in MeCN are presented in Table 3.

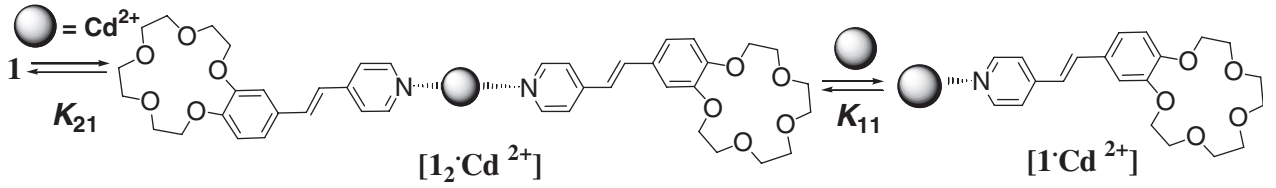

Scheme 4

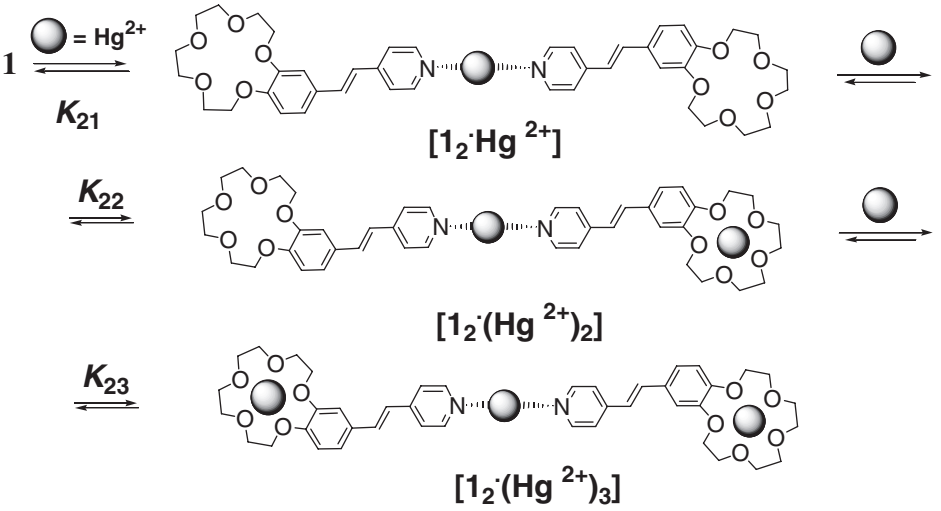

Scheme 5

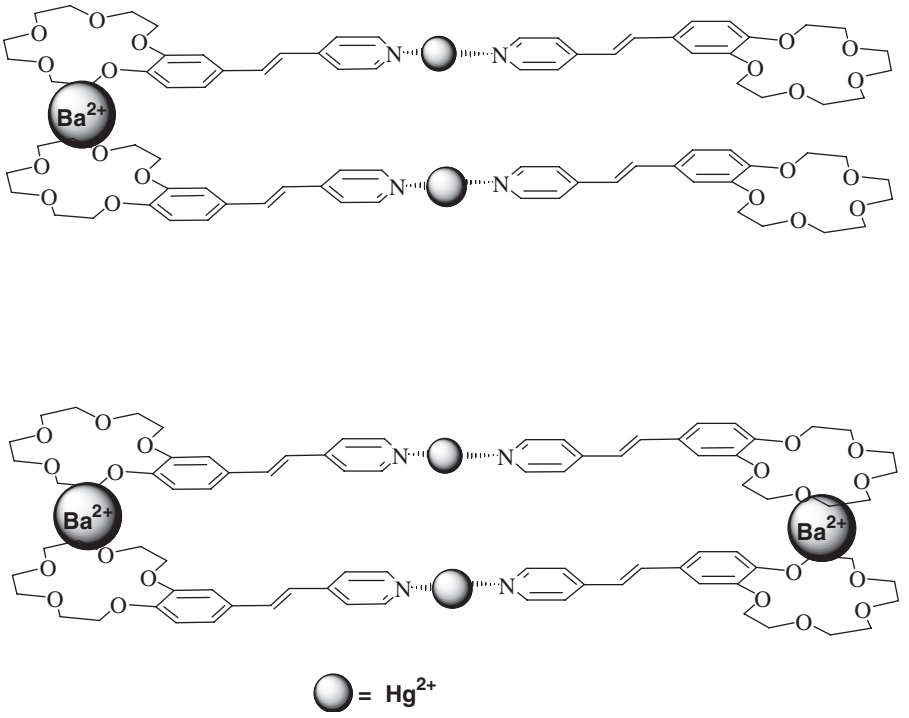

Scheme 6

The fluorescence quantum yield is correlated with the excited state lifetime for all studied complexes and shows an increasing depth of the potential well of the excited *trans* state when the spectra shift to the low-energy side. All kinetics are monoexponential except for the **1** complexes with Cd^{2+} and Hg^{2+}. In presence of these cations, the solution probably contains a mixture of complexes of different stoichiometry. Also, this can be seen in the fluorescence spectrum of **1** with Cd^{2+} (Fig. 3, 2′). At a low concentration of Cd^{2+} ions, both previously discussed complex stoichiometries are present in solution with prevalence of a configuration of two ligands to one cation. With increasing cation concentration, the second configuration (one ligand to one cation) starts to dominate and this gives a nearly Gaussian spectral bandshape of fluorescence (Fig. 3, 3′).

Table 3. Steady-state and time-resolved fluorescence data for **1** and its complexes with Mg^{2+}, Ba^{2+}, Cd^{2+}, Hg^{2+}, H^+ in MeCN

Compound	λ^{fl} (nm)	φ^{fl}	τ_{fl} (ps)
1	408	0.01	49
1·Mg^{2+}	384	0.0073	17
$\mathbf{1}_2$·Ba^{2+}	407	0.0094	24
$\mathbf{1}_2$·Cd^{2+}	485	0.042	115 and 328
1·Cd^{2+}	480	0.027	
$\mathbf{1}_2$·Hg^{2+}	540	0.028	56 and 320
$\mathbf{1}_2$·$(Hg^{2+})_2$ and $\mathbf{1}_2$·$(Hg^{2+})_3$	552	0.037	
[$\mathbf{1}_4$·$(Ba^{2+})_2$ $(Hg^{2+})_2$]	520	0.019	44 and 320
1·H^+	553	0.047	320

The fluorescence Stokes shift varies for different complexes. The lowest shift is observed for the complex with Mg^{2+}, 5600 cm^{-1}, and the highest for protonated complex, 7600 cm^{-1}. The Stokes shift increases when the absorption (and consequently emission) spectral position shifts to the low-energy side. These variations of Stokes shift are in agreement with our discussion above about the charge transfer (and consequently dipole moment) variations for different complexes.

X-ray analysis of the complex [1·Co(NO$_3$)$_2$]

Molecular and crystal structures of the $Co(NO_3)_2$ complex with **1** were determined by x-ray structural analysis. The compound represents a centrosymmetric octahedral aqua Co(II) complex of composition $[Co(H_2O)_4(\mathbf{1})_2]^{2+}2(NO_3)^-$. The structure of the complex cation and the atom numbering scheme are shown in Fig. 5. Two opposite octahedral positions are occupied by the N(1) nitrogen atoms of the crown ether dye molecules and the other four by water molecules. The complex situated at the symmetry centre bears two positive charges and, accordingly, the crystal contains one nitrate group in a general position per one centrosymmetric complex cation.

Selected bond lengths and bond angles in the crown ether dye ligand are given in Table 4.

The Co—N(1), Co—O(1) and Co—O(2) bond distances are 2.130(4), 2.088(3) and 2.094 Å, respectively. The O—Co—O bond angles are 91.5 and 88.5(2)°.

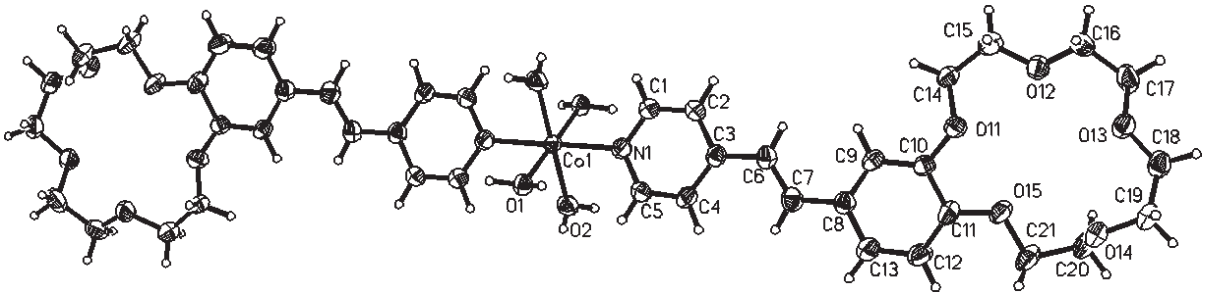

Figure 5. Crystal structure of compound $[Co(H_2O)_4(\mathbf{1})_2]^{2+}2(NO_3)^-$. Molecular structure of **1** with thermal ellipsoids at the probability level of 50% and atom numbering scheme are presented. The atoms of only crystallographically independent part of the molecule are indicated

The conjugated moiety of ligand **1** is nearly planar. The dihedral angle between the pyridine and ethylene fragments is 7.2° and that between the ethylene group and benzene ring is 10.1°.

The pyridine fragment of the ligand exhibits a pronounced bond length redistribution corresponding to a contribution of the *para*-quinoid structure. Actually, two opposite bonds, C(1)—C(2) and C(4)—C(5), are shortened [1.372(7) and 1.369(7) Å] compared with the C(2)—C(3) and C(3)—C(4) bonds [1.404 and 1.409(7) Å]. The bond lengths at the nitrogen atom are 1.343(7) and 1.355(7) Å. The endocyclic angles at the N(1) and C(3) atoms are reduced to 116.6(4) and 116.5(5)°, whereas the angles at the C(1) and C(5) carbon atoms nearest to the nitrogen atom are increased to 123.2(5) and 124.1(5)°, respectively. The C(6)—C(7) ethylene bond length is 1.342(8) Å, which is not far from the standard value of the double bond (1.33 Å). The C(3)—C(6) bond length [1.462(7) Å] is shorter than the C(7)—C(8) bond length, in accordance with the *para*-quinoid pattern of the pyridine ring.

The benzene ring of the benzocrown system also exhibits geometric distortion. The C(9)—C(10) bond length [1.378(7) Å] is shorter than those of the two adjacent bonds C(10)—C(11) and C(8)—C(9) [1.415(7) and 1.409(8) Å], whereas the second half of the benzene ring, C(11)—C(12)—C(13)—C(8), reveals complete bond length delocalization [1.383(8), 1.390(8) and 1.389(8) Å, respectively]. The second peculiarity of the benzocrown ether molecules is a significant distortion of the O—C_{Ph}—C_{Ph} bond angles. Actually, two angles, O(11)—C(10)—C(11) and O(15)—C(11)—C(10), included in the macrocycle are reduced [114.6(4) and 114.9(5)°] and two others, O(11)—C(10)—C(9) and O(15)—C(11)—C(12), are increased [124.5(5) and 126.3(5)°]. These geometric peculiarities were observed previously for series of molecules containing similar benzocrown ether moieties.[28–31] They are apparently

Table 4. Selected bond lengths (Å) and angles (°) in $[Co(H_2O)_4(\mathbf{1})_2]^{2+}2(NO_3)^-$

Co(1)—N(1)	2.130(4)	C(7)—C(8)	1.475(7)
Co(1)—O(1)	2.088(3)	C(8)—C(9)	1.409(8)
Co(1)—O(2)	2.094(4)	C(9)—C(10)	1.378(7)
N(1)—C(1)	1.343(7)	C(10)—C(11)	1.415(7)
N(1)—C(5)	1.355(7)	C(11)—C(12)	1.383(8)
C(1)—C(2)	1.372(7)	C(12)—C(13)	1.390(8)
C(2)—C(3)	1.404(7)	C(13)—C(8)	1.389(8)
C(3)—C(4)	1.409(8)	O(11)—C(10)	1.372(6)
C(4)—C(5)	1.369(7)	O(11)—C(14)	1.431(6)
C(3)—C(6)	1.462(7)	O(15)—C(11)	1.367(7)
C(6)—C(7)	1.342(8)	O(15)—C(21)	1.430(6)
O(1)—Co(1)—O(2)	91.5(2)	C(3)—C(6)—C(7)	124.3(5)
O(1)—Co(1)—N(1)	90.6(2)	C(6)—C(7)—C(8)	125.6(5)
O(2)—Co(1)—N(1)	89.0(2)	C(9)—C(10)—O(11)	124.5(5)
Co(1)—N(1)—C(1)	122.2(3)	C(11)—C(10)—O(11)	114.6(4)
Co(1)—N(1)—C(5)	121.2(3)	C(12)—C(11)—O(15)	126.3(5)
C(1)—N(1)—C(5)	116.6(4)	C(10)—C(11)—O(15)	114.9(5)
N(1)—C(1)—C(2)	123.2(5)	C(10)—O(11)—C(14)	119.8(4)
N(1)—C(5)—C(4)	124.1(5)	C(11)—O(15)—C(21)	117.4(5)
C(1)—C(2)—C(3)	120.3(5)	C(15)—O(12)—C(16)	113.8(5)
C(5)—C(4)—C(3)	119.2(5)	C(17)—O(13)—C(18)	111.6(4)
C(2)—C(3)—C(4)	116.5(5)	C(19)—O(14)—C(20)	113.6(4)

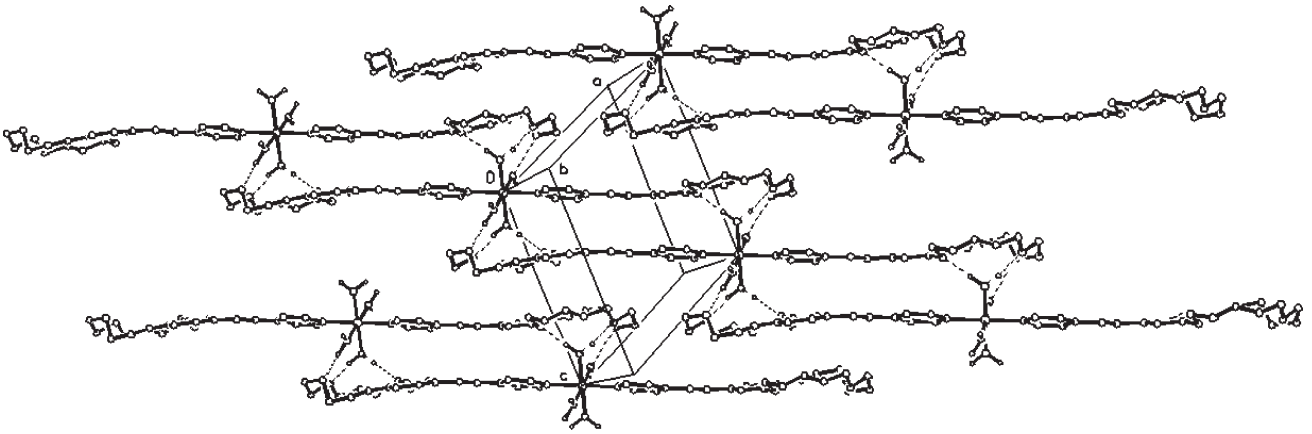

Figure 6. Fragment of crystal packing of doubly-charged cations of compound $[Co(H_2O)_4(\mathbf{1})_2]^{2+}2(NO_3)^-$

due to conjugation of a lone electron pair occupying the p-orbital of each of the oxygen atoms bonded to the benzene ring. The bond angles at the O(11) and O(15) atoms [119.8(4) and 117.4(5)°, respectively] imply their sp^2 hybridization. The other macrocyclic oxygens have the sp^3 hybridization; the angles at the O(12), O(13) and O(14) atoms are 113.8(5), 111.6(4) and 113.6(4)°, respectively.

In the crystal form, the complex cations form infinite staircase-like chains due to hydrogen bonds formed by coordinated water molecules with crown ether moieties of the adjacent molecules (Fig. 6).

The coordinated water molecule $O(1)H_2$ participates in two hydrogen bonds with the O(11) and O(13) atoms of the adjacent molecule. The H···O distances are 1.83 and 1.87 Å and the angles at the hydrogen atoms are 172 and 159°, respectively. The second coordinated molecule, $O(2)H_2$, is involved in only one hydrogen bond, with the O(14) atom of the adjacent molecule. The parameters of this H-bond are 1.90 Å and 161°.

In these chains, the ethylene fragments of the adjacent molecules turned out to be in close vicinity to each other and are in a strictly parallel orientation because they are related through symmetry centres. Projection of the fragment of the chain on to the plane of one C_{Ph}—C═C—C_{Ph} fragment is shown in Fig. 7. It can be seen that the conjugated fragments form a parallel displaced mutual arrangement typical of stacking interactions,[32,33] with a rather short distance [3.499(8) Å] between the atoms of the ethylene group. Such an arrangement is favourable for photochemical [2 + 2]-cycloaddition.

CONCLUSIONS

These optical and x-ray experiments showed the possibility of studying the binding of receptor **1** with metal cations through the participation of two centres: the crown ether moiety and the heterocyclic part. The centres possess different selectivities to metal cations, and the optical response on complex formation also differ for two binding sites. The metal cations studied can be divided into three groups. Alkaline earth metal cations form complexes with the crown ether centre, H^+, Co^{2+}, Cd^{2+} prefer the coordination with the N-atom of the heterocyclic part and Hg^{2+} cations form complexes through coordination with both binding centres (Scheme 7). The importance of the obtained results is that they allow the creation of supramolecular assemblies of different architectures based on crown-containing 4-styrylpyridine. The investigation can also be considered useful for the development of promising fluorescent sensors on metal cations.

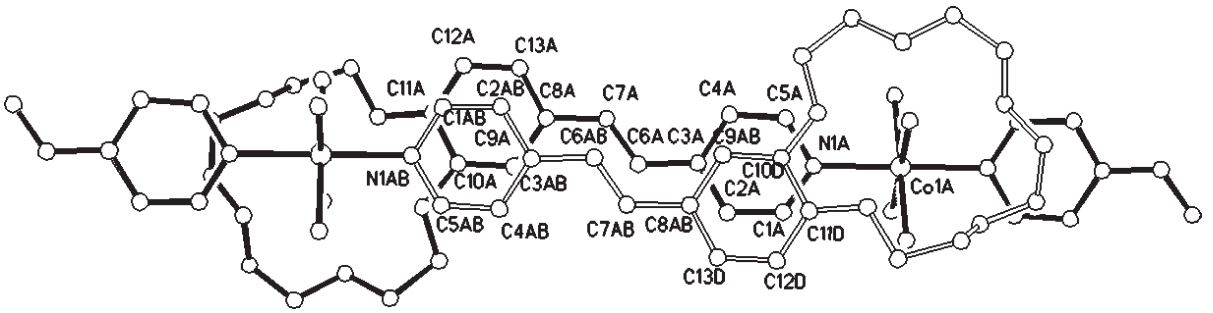

Figure 7. Mutual arrangement of two adjacent conjugated fragments of a hydrogen-bonded chain

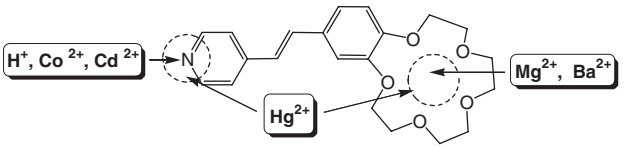

Scheme 7

EXPERIMENTAL

Materials

Anhydrous MeCN, $Mg(ClO_4)_2$, $Ba(ClO_4)_2$, $Cd(ClO_4)_2$, $Hg(ClO_4)_2$ and $Co(NO_3)_2$ (Aldrich) were used as received. Solutions of dye **1** was prepared and used in red light.

Synthesis and NMR study

^{1}H NMR spectra were recorded on a Bruker DRX500 instrument (500.13 MHz) for solutions in CD_3CN, the solvent being used as the internal reference, 1.96 ppm for ^{1}H; 2D homonuclear NOESY spectra were used to assign the proton and carbon signals.

Synthesis of (*E*)-**1**. A mixture of 4-methylpyridine (15 mmol), 4′-formylbenzo-15-crown-5 ether (3 mmol) and *t*BuOK (4.5 mmol) in 5 ml of anhydrous DMF was kept at ambient temperature for 24 h. After addition of distilled water (20 ml), the product was extracted with benzene or CH_2Cl_2 (4×30 ml). The product **1** was purified by column chromatography on silica gel (eluent: benzene–EtOH, 5:1) followed by crystallization from MeOH; yield of **1**, 78%.

4-[(E)-2-(2,3,5,6,8,9,11,12-Octahydro-1,4,7,10,13-benzopentaoxacyclopentadecin-15-yl)-1-ethenyl]pyridine (**1**). M.p. 112–114 °C. ^{1}H NMR (500 MHz, CD_3CN, 25 °C): δ 3.66 (m, 4 H, 2 CH_2O), 3.67 (m, 4 H, 2 CH_2O), 3.84 (m, 4 H, 2 CH_2O), 4.11 (m, 2 H, CH_2OAr), 4.12 (m, 2 H, CH_2OAr), 6.96 (d, 1 H, C(5′)-H, $^3J_{H,H} = 8.1$ Hz), 7.05 (d, 1 H, C(b)-H, $^3J_{H,H} = 16.3$ Hz), 7.15 (dd, 1 H, C(6′)-H, $^3J_{H,H} = 8.1$ Hz, $^4J_{H,H} = 1.2$ Hz), 7.23 (s, 1 H, C(2′)-H), 7.38 (d, 1 H, C(a)-H, $^3J_{H,H} = 16.3$ Hz), 7.52 (d, 2 H, C(3)-H, C(5)-H, $^3J_{H,H} = 5.7$ Hz), 8.50 (d, 2 H, C(2)-H, C(6)-H, $^3J_{H,H} = 5.7$ Hz). MS (EI, 70 eV): *m*/*z* 371 (31) [M^+], 240 (47), 239 (100), 224 (32), 183 (29), 182 (32), 167 (28), 154 (37), 153 (58), 129 (38), 83 (47). $C_{21}H_{25}NO_5$. Calcd C 67.91, H 6.78, N 3.77; found C 68.04, H 6.76, N 3.66%.

Synthesis of the complex of (*E*)-**1** *with* $Mg(ClO_4)_2$. $Mg(ClO_4)_2$ (0.9 mg, 0.004 mmol) and (*E*)-**1** (1.5 mg, 0.004 mmol) were dissolved in 0.6 ml of CD_3CN in red light. The resulting $[(E)\text{-}\mathbf{1}]\cdot Mg^{2+}$ was used for NMR investigation (500 MHz, CD_3CN, 25 °C): δ 3.67 (m, 8 H, 4 OCH_2), 3.97 (m, 2 H, OCH_2), 4.03 (m, 2 H, OCH_2), 4.18 (m, 2 H, CH_2OAr), 4.53 (m, 2 H, CH_2OAr), 7.17 and 7.51 (2 d, 2 H, C(a)-H, C(b)-H, $^3J_{H,H} = 16.4$ Hz, $^3J_{H,H} = 16.4$ Hz), 7.40 (m, 2 H, C(2′)-H, C(6′)-H), 7.22 (d, 1 H, C(5′)-H, $^3J_{H,H} = 8.3$ Hz), 7.63 (d, 2 H, C(3)-H, C(5)-H, $^3J_{H,H} = 8.4$ Hz), 8.51 (d, 2 H, C(2)-H, C(6)-H, $^3J_{H,H} = 8.4$ Hz).

Synthesis of the complex of (*E*)-**1** with $Ba(ClO_4)_2$. $Ba(ClO_4)_2$ (0.7 mg, 0.002 mmol) and (*E*)-**1** (1.5 mg, 0.004 mmol) were dissolved in 0.6 ml of CD_3CN in red light. The resulting $[(E)\text{-}\mathbf{1}]_2\cdot Ba^{2+}$ was used for NMR investigation (500 MHz, CD_3CN, 60 °C): δ 3.94 (m, 4 H, 2 OCH_2), 4.00 (m, 4 H, 2 OCH_2), 4.13 (m, 4 H, 2 OCH_2), 4.29 (m, 4 H, 2 CH_2OAr), 6.86 (s, 1 H, C(2′)-H), 6.88 (d, 1 H, C(5′)-H, $^3J_{H,H} = 8.3$ Hz), 6.92 and 7.22 (2 d, 2 H, C(a)-H, C(b)-H, $^3J_{H,H} = 16.4$ Hz, $^3J_{H,H} = 16.4$ Hz), 7.19 (d, 1 H, C(6′), $^3J_{H,H} = 8.3$ Hz), 7.27 (d, 2 H, C(3)-H, C(5)-H, $^3J_{H,H} = 8.3$ Hz), 8.39 (d, 2 H, C(2)-H, C(6)-H, $^3J_{H,H} = 8.3$ Hz).

Synthesis of the complex of (*E*)-**1** *with* $Cd(ClO_4)_2$. $Cd(ClO_4)_2$ (0.65 mg, 0.002 mmol) and (*E*)-**1** (1.5 mg, 0.004 mmol) were dissolved in 0.6 ml of CD_3CN in red light. The resulting $[(E)\text{-}\mathbf{1}]_2\cdot Cd^{2+}$ was used for NMR investigation (500 MHz, CD_3CN, 25 °C): δ 3.61 (m, 8 H, 4 OCH_2), 3.77 (m, 4 H, 2 OCH_2), 4.06 (m, 2 H, CH_2OAr), 4.10 (m, 2 H, CH_2OAr), 6.99 (d, 1 H, C(5′)-H, $^3J_{H,H} = 8.2$ Hz), 7.15 (d, 1 H, C(6′)-H, $^3J_{H,H} = 8.2$ Hz), 7.09 and 7.48 (2 d, 2 H, C(a)-H, C(b)-H, $^3J_{H,H} = 16.3$ Hz, $^3J_{H,H} = 16.3$ Hz), 7.28 (s, 1 H, H-2′), 7.68 (d, 2 H, C(3)-H, C(5)-H, $^3J_{H,H} = 5.8$ Hz), 8.58 (d, 2 H, C(2)-H, C(6)-H, $^3J_{H,H} = 5.8$ Hz).

Synthesis of the complex of (*E*)-**1** *with* $Co(NO_3)_2$. $Co(NO_3)_2$ (3.65 mg, 0.02 mmol) and (*E*)-**1** (15 mg, 0.04 mmol) were dissolved in 6 ml of CD_3CN in red light. The resulting $[(E)\text{-}\mathbf{1}]_2\cdot Co^{2+}$ was used for growing crystals. The resulting $[(E)\text{-}\mathbf{1}]_2\cdot Co^{2+}$ was used for NMR investigation (500 MHz, DMSO-d_6, 25 °C): δ 3.61 (m, 8 H, 4 OCH_2), 3.77 (m, 4 H, 2 OCH_2), 4.06 (m, 2 H, CH_2OAr), 4.10 (m, 2 H, CH_2OAr), 6.96 (d, 1 H, C(5′)-H, $^3J_{H,H} = 7.1$ Hz), 7.14 and 7.41 (2 d, 2 H, C(a)-H, C(b)-H, $^3J_{H,H} = 16.0$ Hz, $^3J_{H,H} = 16.0$ Hz), 7.14 (d, 1 H, C(6′)-H, $^3J_{H,H} = 7.3$ Hz), 7.27 (s, 1 H, C(2′)-H), 7.52 (m, 2 H, C(3)-H, C(5)-H), 8.55 (m, 2 H, C(2)-H, C(6)-H).

UV–visible spectra

Preparation of solutions and all experiments were carried out in red light. The fluorescence quantum yield measurements were provided using Specord-M40 and Varian-Cary spectrophotometers and a FluoroLog (Jobin Yvon) spectrofluorimeter. All measured fluorescence spectra were corrected for the non-uniformity of detector spectral sensitivity. 9,10-Diphenylanthracene in cyclohexane ($F = 0.9$, according to Hamai and Hirayama,[34] was used

as a reference for the fluorescence quantum yield measurements.

Equilibrium constant determination

Complex formation of **1** with $Mg(ClO_4)_2$, $Ba(ClO_4)_2$, $Hg(ClO_4)_2$, $Cd(ClO_4)_2$ or $HClO_4$ in acetonitrile at $20 \pm 1\,^{\circ}C$ was studied by spectrophotometric titration. The ratio of **1** to $Mg(ClO_4)_2$, $Ba(ClO_4)_2$, $Hg(ClO_4)_2$, $Cd(ClO_4)_2$ and $HClO_4$ was varied by adding aliquots of a solution containing known concentrations of **1** and of corresponding salt or acid to a solution of **1** alone of the same concentration. The absorption spectrum of each solution was recorded and the stability constants of the complexes were determined using the Hyperquad program.[24]

Time-resolved fluorescence

These studies were undertaken using a spectrograph (Chromex 250) coupled to a streak camera (Hamamatsu 5680 equipped with fast single sweep unit M5676, temporal resolution 2 ps). The fluorescence excitation light pulses were obtained by frequency doubling and tripling of a Ti:sapphire femtosecond laser system (Femtopower Compact Pro) output. All excited-state lifetimes were obtained using depolarized excitation light.

X-ray diffraction analysis

Crystals of the compound suitable for x-ray crystallography were grown by slow evaporation from acetonitrile solutions. The structure was solved by direct methods and refined by full-matrix least-squares on F^2 in anisotropic approximation for all non-hydrogen atoms. The hydrogen atoms were calculated geometrically and refined using the 'riding' model.

The nitrate anion was found to be disordered over two positions situated in the vicinity of a symmetry centre with equal population. Moreover, difference Fourier syntheses revealed a number of residual peaks of electron density interpreted by us as water molecules with partial populations. The occurrence of disordered water molecules of crystallization evidences a rather loose crystal packing at least in the vicinity of crystal arias occupied with crown ether fragments.

The Bruker SAINT program[35] was used for data reduction. SHELXTL-Plus[36] software was used for the structure solution and refinement. Crystallographic data and structure solution and refinement parameters are given in Table 5. Crystallographic data (excluding structure factors) for the structure have been deposited with the Cambridge Crystallographic Data Centre as supplementary publication No. CCDC 245027. Copy of the data can be obtained free of charge on application to CCDC, 12 Union Road, Cambridge CB21EZ, UK [fax: (+44)1223 336 033; e-mail: deposit@ccdc.cam.ac.uk].

Table 5. Crystal data, data collection, structure solution and refinement parameters

Parameter	$[Co(H_2O)_4(\mathbf{1})_2]^{2+}2(NO_3)^{-}\cdot nH_2O$
Empirical formula	$C_{42}H_{58}CoN_3O_{19.70}$
Formula weight	979.04
Crystal size (mm)	$0.30 \times 0.10 \times 0.10$
Crystal system	Triclinic
Space group	$P\bar{1}$
Unit cell dimensions:	
a (Å)	10.3221(8)
b (Å)	10.9142(8)
c (Å)	12.2126(9)
α (°)	98.428(3)
β (°)	105.776(3)
γ (°)	105.752(3)
V (Å^3)	1237.7(2)
Z	1
Density (calc.) (g cm^{-3})	1.314
μ(Mo Kα) (mm^{-1})	0.422
F(000)	516
Diffractometer	Bruker CCD SMART
Temperature (K)	120.0(2)
Radiation, λ (Å)	Graphite monochromatized Mo Kα (0.71073)
θ range (°)	1.78 to 28.00
Index ranges	$-11 \le h \le 13$, $-12 \le k \le 14$, $-15 \le l \le 16$
Reflections collected	7429
Independent reflections	5748 [R(int) = 0.0342]
Absorption correction	Not applied
Data/parameters	5748/332
Goodness-of-fit on F^2	1.052
Final Rs [$I > 2\sigma(I)$]	$R_1 = 0.1022$, $wR_2 = 0.2893$
Rs (all data)	$R_1 = 0.1402$, $wR_2 = 0.3123$
Largest diff. peak and hole (e Å^{-3})	1.258 and −0.618

Acknowledgments

The study was supported by CRDF (Grant RC2-2344-MO-02), RFBR (Projects 02-03-33058 and 03-03-32849), the Russian Academy of Sciences, and the programme 'Integration' of the Ministry for Science and Education of Russia. We thank the Région Aquitaine and the Ministère de l'Education Nationale de la Recherche et da la Technologie for financial support. We also gratefully appreciate discussions with Dr René Lapoyade.

REFERENCES

1. Rettig W, Strehmel B, Schrader S, Seifert H (eds). *Applied Fluorescence in Chemistry, Biology, and Medicine*. Springer: Berlin, 1999.
2. Guilbault GG. *Practical Fluorescence. Theory, Methods and Techniques*. Marcel Dekker: New York, 1973.

3. Krasnovskii BM, Boilotin BM. *Organic Luminescence Materials*. VCH: Weinheim, 1988.
4. Schulman SG. *Molecular Luminescence Spectroscopy. Methods and Application.* Wiley: Chichester, 1993.
5. Czarnic AW (ed). *Fluorescent Chemosensor for Ion and Molecule Recognition*. ACS Symposium Series 358. American Chemical Society: Washington, DC, 1993.
6. Lakowics JR (ed). *Probe Design and Chemical Sensing. Topics in Fluorescene Spectroscopy*, vol. 4. Plenum Press: New York, 1993.
7. Desvergne JP, Czarnik AW (eds). *Chemosensor of Ion and Molecule Recognition*. NATO ASI Series. Kluwer: Dordrecht, 1997.
8. Valeur B, Leray I. *Coord. Chem. Rev.* 2000; **205**: 3–40.
9. Wolfbeis OS. *Fiber Optic Chemical Sensors and Biosensors*, vols. I–II. CRC Press: Boca Raton, FL, 1991.
10. Guilbault GG. *Practical Fluorescence*. Marcel Dekker: New York, 1990.
11. Lehn JM (ed). *Comprehensive Supramolecular Chemistry*. Pergamon Press: New York, 1996.
12. Inoue Y, Gokel GW (eds). *Cation Binding by Macrocycles*. Marcel Dekker: New York, 1990.
13. Druzhinin SI, Rusalov MV, Uzhinov BM, Alfimov MV, Gromov SP, Fedorova OA. *J. Appl. Spectrosc.* 1995; **62**: 69–72.
14. Alfimov MV, Fedorova OA, Gromov SP. *J. Photochem. Photobiol. A* 2003; **158**: 183–198.
15. Rettig W, Majenz W, Lapouyade R, Vogel F. *J. Photochem. Photobiol. A: Chem.* 1992; **65**: 95–110.
16. Veggel FCJM, Verboom W, Reinhoudt DN. *Chem. Rev.* 1994; **94**: 279–299.
17. Cazaux L, Faher M, Lopez A, Picard C, Tisnes P. *J. Photochem. Photobiol. A: Chem.* 1994; **77**: 217–225.
18. Letard JF, Delmond S, Lapouyade R, Braun D, Rettig W, Kreissler M. *Recl. Trav. Chim. Pays-Bas* 1995; **114**: 517–527.
19. Bourson J, Valeur B. *J. Phys. Chem.* 1989; **93**: 3871–3876.
20. Bricks YL, Slominskii JL, Kudinova MF, Tolmachev AI, Rurack K, Resch-Gerger U, Rettig W. *Photochem. Photobiol. A:* 2000; **132**: 193–208.
21. Karunakaran C, Thomas KRC, Shunmugasundaram A, Murugesan R. *J. Inclusion Phenom. Macrocycl. Chem.* 2002; **38**: 233–249.
22. Karunakaran C, Thomas KRC, Shunmugasundaram A, Murugesan R. *J. Chem. Crystallogr.,* 1999; **29**: 413–420.
23. Lipkowski J. In *Inclusion Compounds*, vol. 1, Atwood JL, Davies JE, MacNicol DD (eds). Academic Press: London, 1984; 59–100.
24. Gans P, Sabatini A, Vacca A. *Talanta* 1996; **43**: 1739–1753.
25. Rettig W, Lapouyarde R. In *Topics in Fluorescence Spectroscopy*, vol. 4, Lakowics JR (ed). Plenum Press: New York, 1994; 109.
26. Valeur B, Badaoui F, Bardez E, Bourson J, Boutin P, Chatelein A, Devol I, Larrey B, Lefevre JP, Soulet A. In *Chemosensors of Ion and Molecular Recognition*, Desvergne JP, Czarnik AW (eds). NATO ASI Series. Kluwer: Dordrecht, 1977; 195.
27. Dauhal A, Roshal AD, Organero JA. *Chem. Phys. Lett.* 2003; **381**: 519–525.
28. Gromov SP, Vedernikov AI, Ushakov EN, Kuz'mina LG, Feofanov AV, Avakyan VG, Churakov AV, Alaverdian YS, Malysheva EV, Alfimov MV, Howard JAK, Eliasson B, Edlund UG. *Helv. Chim. Acta* 2002; **85**: 60–81.
29. Fedorova OA, Fedorov YV, Vedernikov AI, Yescheulova OV, Gromov SP, Alfimov MV, Kuz'mina LG, Churakov AV, Howard JAK, Zaitsev SY, Sergeeva TI, Möbius D. *New J. Chem.* 2002; **26**: 543–553.
30. Gromov SP, Dmitrieva SN, Vedernikov AI, Kuz'mina LG, Churakov AV, Strelenko YA, Howard JAK. *Eur. J. Org. Chem.* 2003; **16**: 3189–3199.
31. Fedorov YV, Fedorova OA, Andryukhina EN, Gromov SP, Alfimov MV, Kuzmina LG, Churakov AV, Howard JAK, Aaron JJ. *New J. Chem.* 2003; **27**: 280–288.
32. Janiak C. *J. Chem. Soc. Dalton Trans.* 2000; **21**: 3885–3896.
33. Muller-Dethlefs K, Honza P. *Chem. Rev.* 2000; **100**: 143–167.
34. Hamai S, Hirayama F. *J. Phys. Chem.* 1983; **87**: 83–89.
35. *SAINT, Version 6.02A*. Bruker AXS: Madison, WI, 2001.
36. *SHELXTL-Plus, Release 5.10*. Bruker AXS: Madison, WI, 1997.